VWF Tool based T-J Solar Cell Modeling and Analyzing the Performance

Tapas Chakrabarti, Subir Kumar Sarkar

Abstract—*The solar cell structure is an important factor for realization of better efficiency of a solar cell in conversion of optical source in to electrical source. Using more efficient solar cell, the production cost of solar power can be minimized. Multi-junction Tandem Solar Cells are most effective in conversion of solar energy in to electrical energy. One triple junction III-V tandem solar cell is fabricated in virtual wafer fabrication lab (VWF) in this paper. Three numbers of multi-junction solar cells are designed and fabricated with the III-V materials and stacked on each other with the sequence of descending order of band gap energy and these three cells are inter connected with two tunnel diode. The mesh structure of this fabrication is done in auto-mesh mode which creates cylinders in mesh. The efficiency of this Triple Junction (T-J) solar cell is achieved 30.671% and the Fill Factor of this cell is derived 77%.*

Index Terms— Triple Junction (T-J), Virtual Wafer Fabrication (VWF), Photovoltaic (PV), Current- Voltage curve (I-V curve), Fill Factor (FF), Air Mass ratio (AM), Metal organic vapor phase epitaxial (MOVPE).

I. INTRODUCTION

Application of solar energy is growing rapidly in the field of renewable energy sources, for generation of electric power. The production of electricity from renewable sources is given great importance to avoid the threat of extinction of fossil fuels and control CO_2 level in the environment. To convert the solar radiation in to electricity, Solar Photo Voltaic (PV) modules are used. The PV power generation can be expressed in watts per square meter. The solar radiation conversion efficiency is very poor; hence it is very important to develop models of PV modules. Today, these solar cells are widely used for powering satellites in space, and it is used for terrestrial applications through the use of photovoltaic concentrator systems [1] [2]. It is very important to decrease the PV power production cost, which can be made by increasing the efficiency of solar cell. Modern research in the area of photovoltaic technologies has lead to creation of a huge spectrum of solar cells, which are commonly classified as **three generations**, which differ from one another based on the **material and the processing technology** used to fabricate the solar cells. The material used to make the solar cell determines the basic properties of the solar cell, including the typical range of efficiencies.The multi-junction solar cells are very popular in terms of high efficiency, especially in space exploration mission.

Single solar cells can absorb only a small portion of the solar spectrum. To achieve a higher power density, solar cells with different I-V curves and bandgaps are stacked in order. The top cell has the highest band gap, while the bottom cell has the lowest. This way, a cell absorbs the photons with energy higher than the band gap and produces electric power [3]. At the same time, it allows the lower–energy photons to pass through it. This method is called spectrum separation. In this paper one triple-junction solar cell as InAlGaP /InGaP/InAlGaP– InGaP/GaAs/ AlGaAs/GaAs - InGaP/GaAs/AlGaAs/GaAs with tunnel of GaAs/GaAs has been developed using VWF tool of Silvaco TCAD ATLAS and calibrated various solar photovoltaic physical parameters as J_{SC} , V_{OC} , J_M , V_M , FF and Efficiency are 117.236Amp/m^2, 2.58Volt, 111.80Amp/m^2, 2.10 Volts, 77% and 30.25% respectively. The 2D cell structures are simulated in Silvaco ATLAS.

II. SOLAR CELL MODELING

Fabrication of multi-junction multi layer solar cell modeling using VWF tool of Silvaco TCAD is very similar to fabrication of multi layer individual solar cell [4]. In this process, individual solar cells are to be built up one by one with their characteristics and mechanically stacked on each other of multi-junction cells [5] [6]. The different fabrication techniques are MBE, MOCVD, MOVPE, LPE applicable in physical fabrication, differs the efficiency of the cell [7]. One triple-junctions solar cell [8] is developed with the different type of III-V compound materials [8]. In this cell three numbers individual cells are constructed along with a multi layer tunnel. The solar cell is made up of InAlGaP/InGaP/InAlGaP –InGaP/GaAs/AlGaAs/GaAs - InGaP/GaAs/AlGaAs/GaAs with tunnel of GaAs/GaAs. The Fill Factor, efficiency of this cell is calculated and performance characteristics are analyzed. In figure-1 and 2 the structure of the cell with the material used is given region wise. In figure-3 and 4 the same structure of the cell is simulated in 2-D, in which the doping concentration is reflected region wise. In this fabrication the mesh generation is done as shown in the simulation of figure-3 and figure-4. The solar cell is constructed region wise with the different materials and their Permittivity (ε), Band gap energy Eg (eV) at 300^{0}K, Lattice Constant (α) and the Affinity of the carrier in eV are considered in this fabrication of the cell in VWF Silvaco-Atlas TCAD are given in the table No-1.
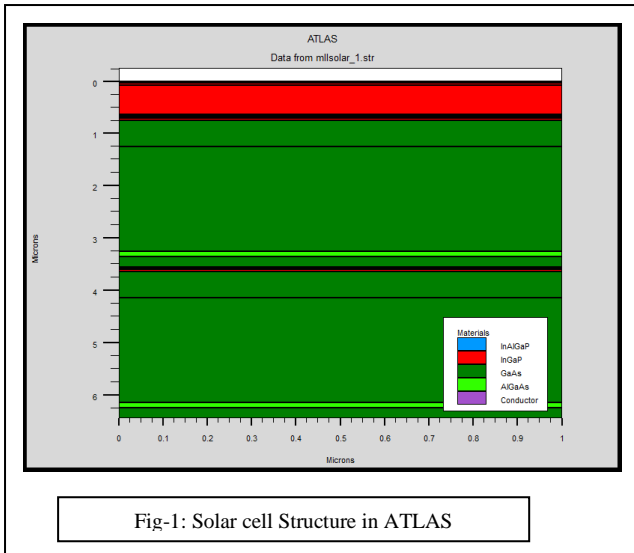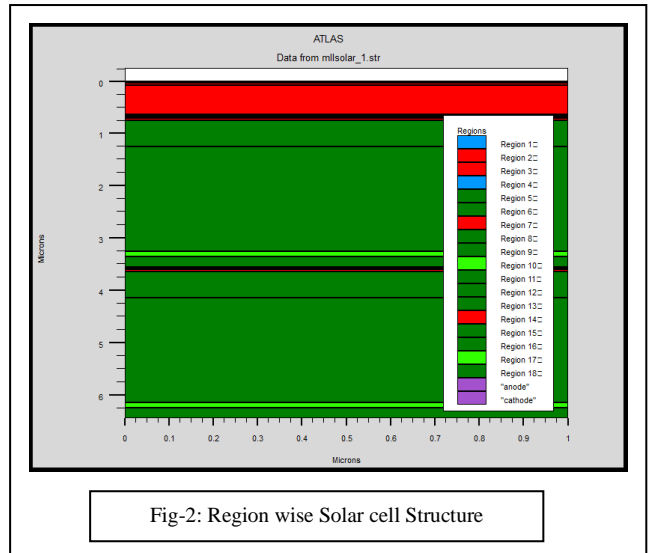
Fig-1: Solar cell Structure in ATLAS
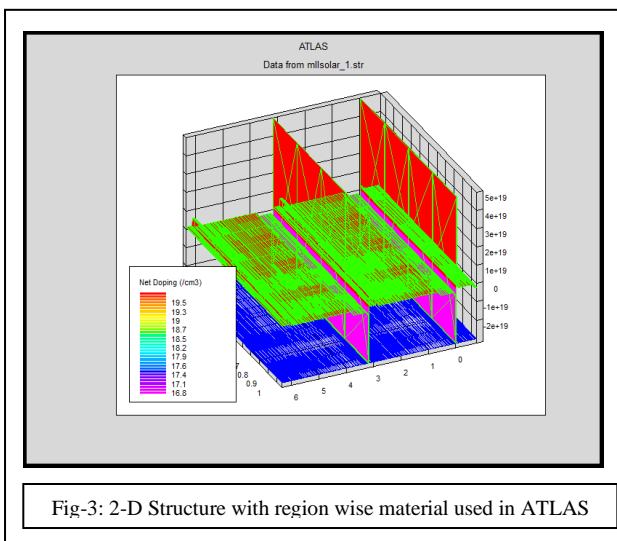
Fig-2: Region wise Solar cell Structure

Fig-3: 2-D Structure with region wise material used in ATLAS
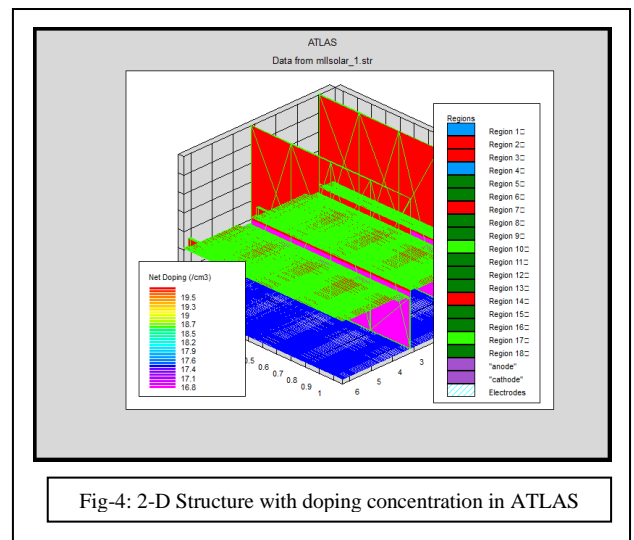
Fig-4: 2-D Structure with doping concentration in ATLAS

III. DRIFT DIFFUSION MODEL

The solar photovoltaic cell models discussed above are being integrated within the advance software Silvaco ATLAS. In this paper the 2D simulator tool is used, where a large data base of the semiconductor materials properties are incorporated. These mathematical models in ATLAS, set of fundamental equations are considered, which link together, the electrostatic potential and carrier densities within some simulator domain. These equations, which are solved inside the device simulator, derived from Maxwell's law and consist of Poisson's equation. [9]Poisson's equation relates the electrostatic potential to the space charge density

$$div(\varepsilon \nabla \varphi) = -\rho \ \ldots\ldots\ldots\ldots\ldots \ (1)$$

where, φ = electrostatic potential

ε = permittivity

ρ = space charge density

the electric field is obtained from the gradient of the potential:

$$\vec{E} = -\nabla \varphi \ \ \ldots\ldots\ldots\ldots\ldots\ldots\ldots\ldots\ldots \ (2)$$

Hence, the current equation governed by the Poisson's equation of electrostatic potential is as:

$$\nabla \varepsilon \nabla \varphi = q(n - p - C) \ \ldots\ldots\ldots\ldots\ldots\ldots\ldots \ (3)$$

where, doping, $C = N_D^+ - N_A^-$ [1]

The continuity equations for electron and holes are used for drift and diffusion models in this software. The conservation of charge for electrons is represented by the following equation:

$$\frac{\partial n}{\partial t} = \frac{1}{q} div\vec{J_n} + G_n - R_n \ \ \ldots\ldots\ldots\ldots \ (4)$$

And similarly for holes the equation is:

$$\frac{\partial p}{\partial t} = \frac{1}{q} div\vec{J_p} + G_p - R_p \ \ \ldots\ldots\ldots\ldots \ (5)$$

Where n and p are the electron and hole densities in per cubic cm, $\vec{J_n}$ and $\vec{J_p}$ are the electron and hole current densities, G_n and G_p are the generation rates for electrons and holes, R_n and R_p are the recombination rates for electrons and holes, and q is the magnitude of the electron charge. The electron current density we can write as

$$\vec{J_n} = q\mu_n(U_T \nabla n - n\nabla \varphi) \ \ldots\ldots\ldots\ldots\ldots \ (6)$$

And the hole current is

$$\vec{J_p} = -q\mu_p(U_T \nabla p - p\nabla \varphi)$$
$$\ldots\ldots\ldots\ldots\ldots\ldots\ldots\ldots\ldots(7)$$

Here μ_n and μ_p are the electron and hole mobility respectively, φ is the electrostatic potential

As per Boltzmann statistics the diffusion coefficient correspondingly

$$D_n = \frac{K_B T}{q} \mu_n \text{ .... (8)} \text{ and}$$

$$D_p = \frac{K_B T}{q} \mu_p \text{ .... (9)} \text{ and let, } \frac{K_B T}{q} = U_T$$

So the equation (8) & (9) can be rewritten as

$$D_n = U_T \mu_n \quad cm^2/sec \text{ .... (8.1) and}$$
$$D_p = U_T \mu_p \quad cm^2/sec \text{ .... (8.2)}$$

In Figure 5 the wave length versus intensity curve in air mass ratio of (AM1.5) is given, where as the dark current and the photo current curve is given in figure-6.

IV. PERFORMANCE ANALYSIS OF MODELED SOLAR CELL

The solar cell performance has been analyzed on the basis of received output from the Silvaco ATLAS software. The software solved the equation of electrostatic equation and the following parameters are received:

The short circuit current density of the solar cell is $J_{sc} = 117.236 \, e - 12$ ampere per square meter and the open circuit voltage

$$V_{OC} = \frac{n K_B T}{q} \ln \left(\frac{I_L}{I_0} + 1 \right) \text{ .... (9) [4]}$$

where, n is the number of cell, K_B is Boltzmann constant and T is the absolute temperature of cell, I_L is the load current and I_0 is the saturation current of the cell. The open circuit voltage is $V_{OC} = 2.58$ volts. The maximum voltage V_m and maximum current I_m is defined as 2.10 Volts and 7.20 e-10 Amps and the derived maximum current density J_m is 111.80 ampere per square meter.

The equation for I-V curve in the first quadrant is:

$$I = I_0 \left[\exp \left(\frac{qV}{n K_B T} \right) - 1 \right] \text{ .... (10) [4] [10]}$$

The short circuit current (I_{sc}) of the cell is $J_{SC} * area$ of the cell and the maximum Power $P_m = V_{max} * I_{max} = 1.512 * 10^{-10}$ watt.

The Fill Factor of solar cell,

$$FF = \frac{P_{max}}{V_{OC} \cdot I_{SC}} = 0.77 \text{ or } 77\% \text{ .... (11)}$$

The efficiency of the cell =

$$\eta = \left(\frac{V_{OC} \, I_{SC}}{P_{in} \, x \, Area \, of \, the \, cell} * FF \right) \% = 30.25\% \text{ .. (12)}$$

Here we have considered the source of one solar sun with AM 1.5 [11]. The I-V characteristics curve of this triple junction solar cell is drawn in figure-7, from this curve the short circuit current and open circuit voltage is achieved. In figure-8, the available photocurrent with respect to the anode voltage is shown. In the figure-9, the anode voltage versus short circuit current and in figure-10, anode current with respect to anode voltage is shown. The different optimized value of this triple junction solar cell is given in table-2.
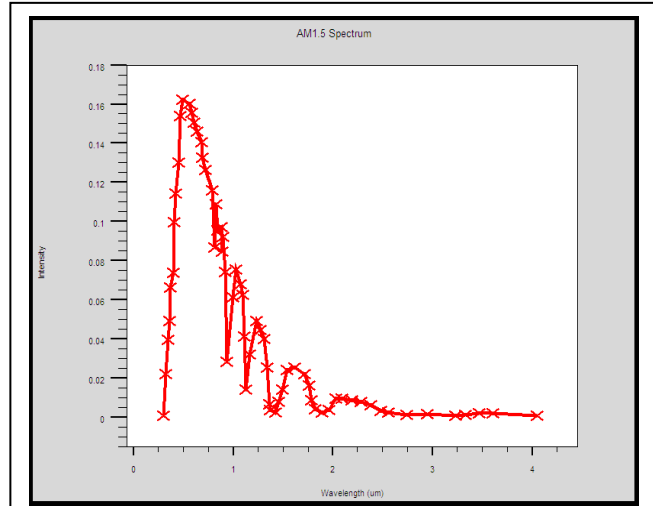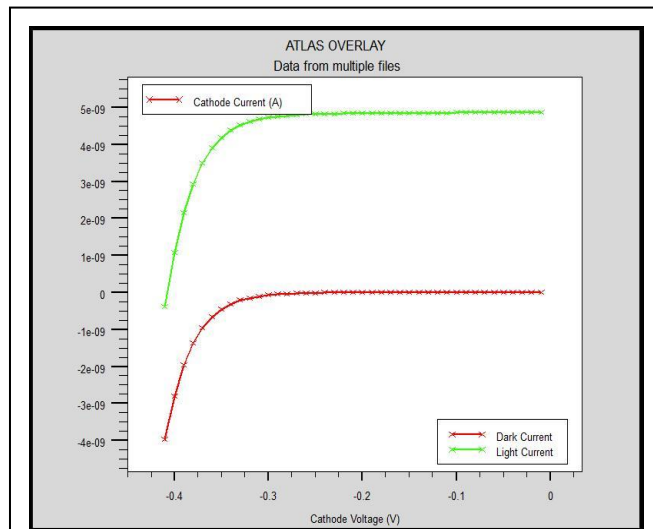

Fig. 5: Wave Length Vs. Intensity in AM1.5

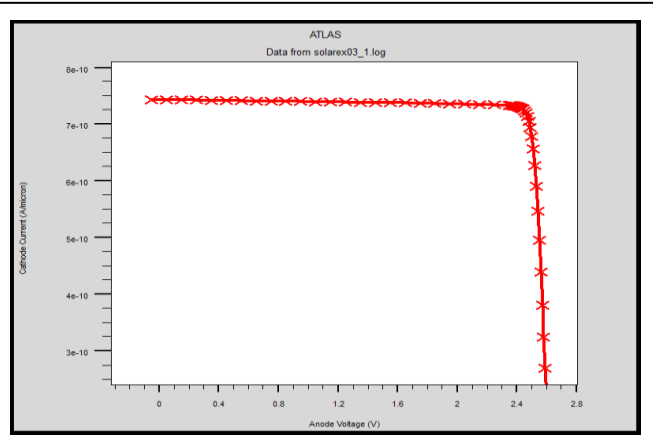**Fig. 6: Dark Current and Photo Current (Cathode Current)**
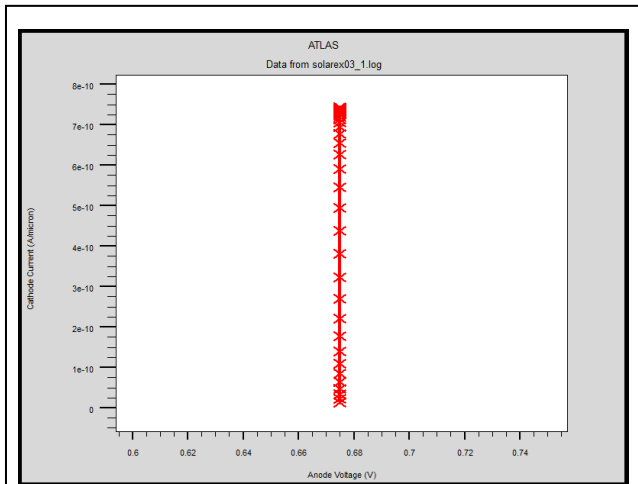

Fig-7: Wave length Vs. Intensity in AM1.5
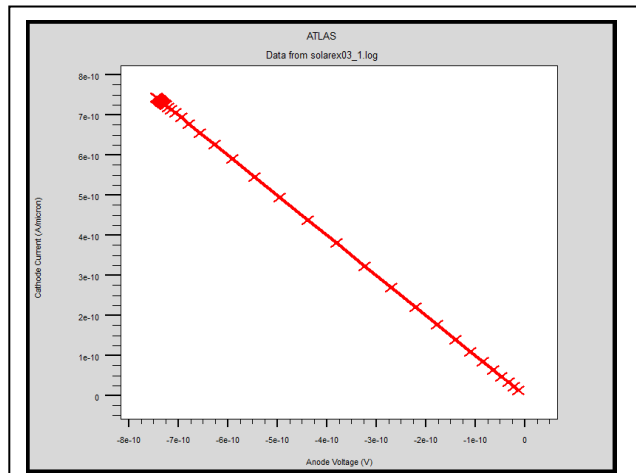
Fig. 8: Wave Length Vs. Intensity in AM1.5

Fig. 10: Wave Length Vs. Intensity in AM1.5

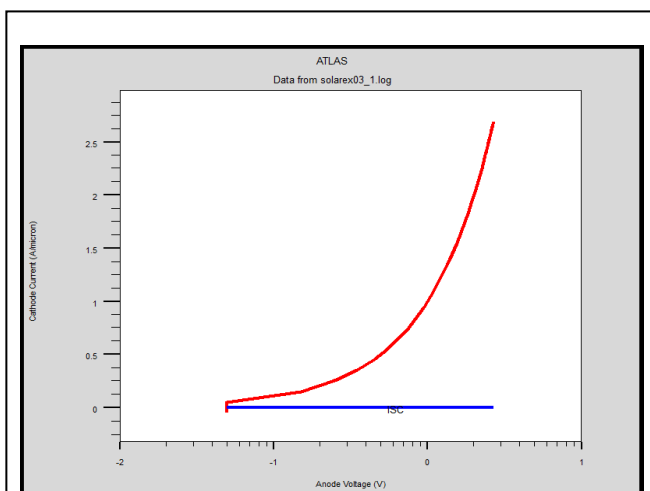**Table-2: Results of T-J solar cell of**

The Parameters	Derived value
J_{sc}	117.236 Amp/m^2
V_{oc}	2.58 Volts
J_{max}	111.80 Amp/m^2
V_{max}	2.10 volts
P_{max}	1.512 e-09 watt
Size of cell	1.00μm x6.44μm
P_{input}	1solar in AM1.5
FF	77%
Efficiency(η)	30.67%

InAlGaP/InGaP/GaAs/AlGaAs

Structure of solar cell	Efficiency
AlGaAs/GaAs dual junction (DJ) solar cells [11]	25%
InGaP/GaAs dual junction (DJ) solar cell [12]	28.69%
InAlGaP/InGaP/GaAS dual junction (TJ) solar cell [modeled]	30.671

Table-3: Comparison of DJ and modeled TJ Solar Cell

Fig. 9: Wave Length Vs. Intensity in AM1.5

Table-1: Parameters used in Design

Regions of the modeled Tandem cell	Region wise Material	Prmittivity (ε) of the material	Bandgap Energy of the material. Eg (eV) at 300^0 K	Lattice constant α (Å)	Affinity (eV) of the used material
1	InAlGaP	11.7	2.3	5.5	4.2
2	InGaP	11.6	1.9	5.65	4.16
3	InGaP	11.6	1.9	5.65	4.16
4	InAlGaP	11.7	2.3	5.65	4.2
5	GaAs	13.1	1.42	5.65	4.07
6	GaAs	13.1	1.42	5.65	4.07
7	InGaP	11.6	1.9	5.65	4.16
8	GaAs	13.1	1.42	5.65	4.07
9	GaAs	13.1	1.42	5.65	4.07
10	AlGaAs	11.0	1.8	5.64	4.1
11	GaAs	13.1	1.42	5.65	4.07
12	GaAs	13.1	1.42	5.65	4.07
13	GaAs	13.1	1.42	5.65	4.07
14	InGaP	11.6	1.9	5.65	4.16
15	GaAs	13.1	1.42	5.65	4.07
16	GaAs	13.1	1.42	5.65	4.07
17	AlGaAs	11.0	1.8	5.64	4.1
18	GaAs	13.1	1.42	5.65	4.07

V. CONCLUSION

The virtual fabrication technique has been adopted and the structure has been fabricated with the auto-mesh and the electrical parameters are calculated on the basis of simulation results of this structure in the virtual wafer fabrication environment. The efficiency of the T-J solar cell is 30.671%, which is better than the double junction solar cell. The comparison of D-J solar cell and T-J solar cell is given in table-3. The efficiency of modeled T-J solar cell is not satisfactory as the targeted T-J solar cell efficiency is beyond 40% since long back [1][8]. The efficiency of solar cell can be developed more with the modification of meshing and fabrication techniques.

49

The antireflection coating and texturisation of the upper surface will increases the efficiency of the solar cell. The appropriate material choosing is another criterion for the better efficiency of a solar cell. The band gap energy should be sequential to get more efficiency for converting optical source in to electrical output. The tunnel diode is also a very important part, in connection of efficiency of the cell. Here we have use the GaAs material for tunneling.

REFERENCES

1. Hector Cotal, Chris Fetzer, Joseph Boisvert, Geoffrey Kinsey, Richard King, Peter Hebert, Hojun Yoon and Nasser Karam, "III–V multijunction solar cells for concentrating photovoltaics", Energy Environ. Sci., 2009, 2, 174–192.
2. A.W. Bett, F. Dimroth, G. Stollwerck, O.V. Sulima, "III-V compounds for solar cell applications", Appl. Phys. A 69, 119–129 (1999), Springer-Verlag 1999.
3. H. W. Wang, M. A. Tsai1, H. C. Chen1 , Y. L. Tsai1, P. C. Tseng1, C. Y. Jang1, Peichen Yu1, H. C. Kuo, "Efficiency Enhancement InGaP/GaAs dual junction solar cell with sub-wavelength antireflection nanorod arrays**",** IEEE conference 2010, 978-1-4244-5892.
4. Khomdram Jolson Singh, Subir Kumar Sarkar, "Highly efficient ARC less InGaP/GaAs DJ solar cell numerical modeling using optimized InAlGaP BSF layers", Opt. Quant Electron of Springer, November,2011.
5. Melissa J. Archer[1], Daniel C.Law[2], "GaInP/GaAs Dual junction solar cells on Ge/Si Epitaxial templates", IEEE conference 2008, 978-1-4244-1641.
6. Jose L. Cruz-Campa, Gregory N. Nielson, Anthony L. Lentine, Anton A. Filatov, Paul J. Resnick, Carlos A, "Fabrication of Lattice Mismatched Multijunction Photovoltaic Cells Using 3D Integration Concepts", IEEE conference 2011,978-1-4673-0066-7/12.
7. S. A. Ringel,1,2,3 J. A. Carlin,3 T.J. Grassman,1,2 B. Galiana,1,3 A.M. Carlin,1 C. Ratcliff, " Ideal GaP/Si Heterostructures Grown by MOCVD: III-V/Active-Si Subcells, Multijuntions, and MBE-to-MOCVD III-V/Si Interface Science", IEEE conference 2013, 978-1-4799-3299-3/13.
8. J. M. Olson, D. J. Friedman and Sarah Kurtz, "High-Efficiency III-V Multijunction Solar Cells", Handbook of Photovoltaic Science and Engineering. John Wiley & Sons, Ltd ISBN: 0-471-49196-9, Edited by A. Luque and S. Hegedus.
9. Alexander Fedoseyeva, Timothy Balda, Ashok Ramana, Seth Hubbardb, David Forbesb, and Alexander Freundlich, "Detailed physics based modeling of triple-junction InGaP/GaAs/Ge solar cell", proceedings.spiedigitallibrary.org/ on 04/29/2014.
10. Loredana Cristaldi, Senior Member, IEEE, Marco Faifer, Member, IEEE, Marco Rossi, Student Member, IEEE and Ferdinanda Ponci, Senior Member, IEEE, "A Simple Photovoltaic Panel Model: Characterization Procedure and Evaluation of the Role of Environmental Measurements.", IEEE Transactions on Energy conversion, Vol.27, No.4, December2012.
11. T.V. Torchynska, G.P. Polupan, "III-V material solar cells for space application", Semiconductor Physics, Quantum Electronics & Optoelectronics. 2002. V. 5, N 1. P. 63-70.
12. Rao Tatavarti, G. Hillier, G. Martin, A. Wibowo, R. Navaratnarajah, F. Tuminello, D. Hertkorn, "Lightweight, low cost InGaP/GaAs dual junction solar cells on 100 mm epitaxial liftoff (ELO) wafers", IEEE conference 2009, 978-1-4244-2950.